Dynamical coherent control of photocurrent in bulk GaAs at room temperature

Hirokazu Tahara and Yoshihiko Kanemitsu
Institute for Chemical Research, Kyoto University, Uji, Kyoto 611-0011, Japan
(Received 17 September 2014; revised manuscript received 11 December 2014; published 22 December 2014)

We report coherently controlled photocurrent at room temperature in subpicosecond dynamics. The photocurrent intensity shows a periodic change depending on the time interval between the phase-locked pulses. We identify the carrier generation due to shallow acceptors in bulk GaAs by measuring the photocurrent beat period. The non-instantaneous photocurrent beat expresses the ultrafast coherent dynamics, including the dephasing process of the photogenerated carriers. We also demonstrate photocurrent direction control through manipulation of the localized states.

DOI: 10.1103/PhysRevB.90.245203 PACS number(s): 72.40.+w, 71.55.Eq, 78.47.J−

I. INTRODUCTION

Recently, there has been increasing interest in the fundamental understanding and controlling of photon-to-current conversion in optical and materials science. Photoinduced carrier generation in semiconducting materials is an essential process that determines photovoltaic device efficiency. Si, GaAs, quaternary compound semiconductors, and organic molecules have been extensively investigated to obtain highly efficient solar cells [1–3]. Sophisticated structures, e.g., nanostructures and multijunctions, have also been developed [4–6]. To enhance the efficiency of these photovoltaic devices, the fundamental mechanisms of unique carrier generation processes, e.g., multiple exciton generation, singlet fission, and carrier upconversion, are being examined [7–13]. The understanding of the fundamental carrier generation mechanisms is becoming increasingly important, because of its application in a wide variety of materials and structures.

Photocurrent spectroscopy is one of the most versatile techniques for understanding the intrinsic nature of photogenerated carriers. However, in conventional photocurrent measurements, it is difficult to measure ultrafast dynamics within the picosecond time domain. In addition, ultrafast coherent dynamics in carrier generation processes have rarely been investigated at room temperature. Therefore, it is necessary to develop techniques for measuring ultrafast photocurrent dynamics with a view to understanding microscopic photocurrent mechanisms.

Although control of ultrafast photocurrent dynamics has not been demonstrated, microscopic dynamics can be controlled in all-optical measurements. For example, the phase-lock technique for multiple pulses has been used to control and analyze the coherent dynamics of exciton systems in semiconductors at liquid helium temperature [14–18]. This control is effective only at low temperatures, because excitons become unstable and free carriers are generated at room temperature. The measurement of coherently controlled photocurrent is expected to directly give us a fundamental understanding of carrier generation, including coherent processes, but this technique is rarely used for characterization of material properties. This approach should be established as it can be a powerful tool for the analysis of photocurrent dynamics in the ultrafast time domain, which cannot be achieved in a steady-state photocurrent control [19–21].

In this paper, we report the coherent control of photocurrent in the subpicosecond time domain. The photocurrent exhibits beat signals depending on the time interval between the excitation pulses, which is a photocurrent phenomenon caused by controlling the carrier generation processes. We then explain a method of determining the origin of the photocurrent generation from the photocurrent beat. This is the first demonstration of free-carrier-generation site characterization in the time domain at room temperature. We also demonstrate that the photocurrent direction can be coherently controlled using this technique.

II. EXPERIMENTAL DETAILS

The sample used in this study was a semi-insulating GaAs bulk crystal. To measure photocurrent, a gold (silver) contact was deposited on the front (back) surface. The experimental setup is shown schematically in Fig. 1. Excitation pulses were generated by a mode-locked Ti:sapphire laser with a pulse duration of 56 fs and a repetition rate of 93 MHz, while the phase-locked pulses were generated by actively stabilizing the optical length of a Michelson interferometer [14–18]. Here, the pulse interference was monitored through a monochromator and stabilized by a piezoelectric actuator to yield constructive (in-phase) or destructive (out-of-phase) interference at the center wavelength of the excitation pulses. The in-phase or out-of-phase interference was controlled by the optical length of the interferometer on a subwavelength scale. The phase-locked pulses separated by a time delay were sent into the sample; the photocurrent signals were measured as a function of the delay time, which was controlled by a stepping-motor-driven delay stage. Here, the phase-locked pulses were divided by a beam splitter in front of the sample. The interference intensity of the pulses was simultaneously measured by a broadband Si photodetector.

III. RESULTS AND DISCUSSION

The interference intensity of the excitation pulses is shown in Fig. 2(a), where the excitation wavelength was set to 860 nm. Since the phase lock was performed for the center wavelength of the pulses, the interference intensity is maximal (minimal) for the in-phase (out-of-phase) condition, within the pulse overlap. The experimental results of the photocurrent measurements are shown in Fig. 2(b), where a bias voltage of −0.5 V, measured from the front electrode, was applied on the back electrode. The photocurrent signals were measured

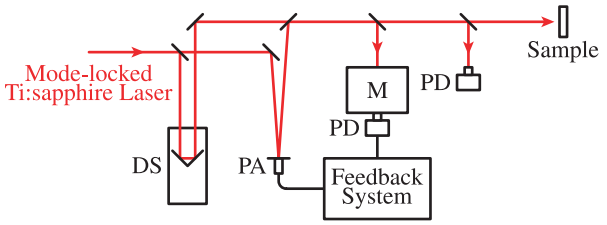

FIG. 1. (Color online) Schematic of the experimental setup. DS: delay stage, PA: piezoelectric actuator, M: monochromator, and PD: photodetector.

simultaneously with the interference of phase-locked pulses shown in Fig. 2(a). In contrast to the monotonic changes in the interference intensity, the drastic changes depending on the delay time were observed in the photocurrent measurement. It is apparent that the current exhibits beat signals with a period of 88 fs under both the in-phase and out-of-phase conditions. The photocurrent beat for the out-of-phase condition is the reverse of that generated under the in-phase condition; it should be noted that the beat disappears under the random-phase condition, where a random phase was created by vibrating a piezoelectric actuator randomly. These results show that the photocurrent beat is sensitive to the relative phase between the excitation pulses. The full width at half maximum (FWHM) of the photocurrent beat decay was found to be 348 ± 8 fs, while the FWHM of the interference intensity of the phase-locked pulses, shown in Fig. 2(a), was measured to be 111.5 ± 0.6 fs. Since the photocurrent beat decay is more than three times as long as the duration of the interference, it is found that the photocurrent beat decay expresses the coherent dynamics of the photoexcited carriers.

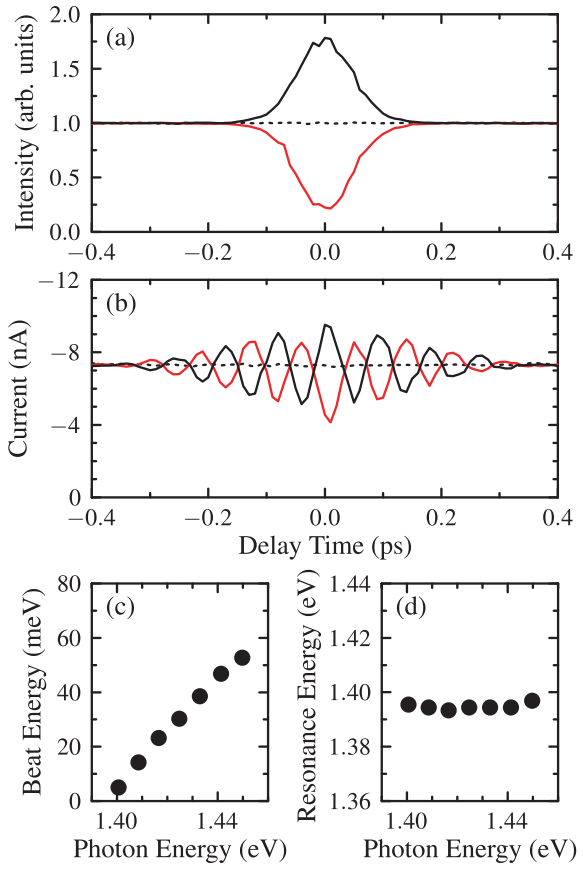

FIG. 2. (Color online) (a) Interference intensity of phase-locked pulses and (b) current as a function of the delay time. Black (red) solid lines indicate results under the in-phase (out-of-phase) condition. Dotted lines represent results under the random-phase condition. (c) Beat energy and (d) resonance energy of photocurrent beat component as a function of excitation energy. The experimental errors are smaller than 0.2 meV.

We also measured the excitation energy dependence of the photocurrent beat. Here, the excitation energy corresponds to the phase-locked energy, because the phase lock was performed for the center energy of the excitation pulses. The interference intensity for each excitation energy shows an interference similar to that shown in Fig. 2(a). The energy corresponding to the beat frequency, called the beat energy in this paper, is shown in Fig. 2(c). Since the beat energy linearly increases with excitation energy, it indicates that the beat period is determined by the detuning from a resonance energy which generates the photocurrent beat. On the basis of this consideration, the resonance energy $\hbar\omega_{\rm res}$ can be obtained from $\hbar\omega_{\rm res} = \hbar\omega_{\rm ex} - \hbar\omega_{\rm beat}$, where the excitation energy and the energy corresponding to the beat frequency are denoted by $\hbar\omega_{\rm ex}$ and $\hbar\omega_{\rm beat}$, respectively. The resonance energy is independent of the excitation energy, as shown in Fig. 2(d), and this independence shows that the resonance energy of the carriers contributing to the photocurrent is accurately obtained from the photocurrent beat measurement. Here, the resonance energy was determined to be 1394 meV at room temperature.

In order to clarify the origin of the photocurrent, we measured the temperature dependence of the photocurrent beat. The beat period becomes long with decreasing temperature, as shown in Fig. 3(a), where the period changes from 104 to 181 fs with decreasing temperature from 279 to 240 K for the excitation wavelength of 860 nm. This extension of beat period shows that the resonance energy exhibits a temperature-dependent blueshift. We then measured the photoluminescence (PL) spectra to observe the resonance peak estimated to be 1394 meV at room temperature. For bulk materials, PL spectroscopy is widely used to characterize impurity states, because the PL spectrum is very sensitive to small amounts of impurities compared to conventional steady-state absorption and reflection spectra [22,23]. However, a resonance peak is not observed at the estimated energy of 1394 meV in the PL spectrum as shown in Fig. 3(b). The peak due to the band-to-band transition is only observed at room temperature (298 K). In contrast, there are two peaks at a low temperature of 10 K. The peaks at 1512 and 1494 meV correspond to the neutral acceptor bound exciton and band acceptor peaks, respectively, which have been reported as the peaks due to carbon acceptors [24]. The band acceptor peak shows that the acceptor level is lower than the band gap energy by 26 meV. It is expected that the photocurrent beat is caused by the acceptor state, because the resonance energy estimated from the photocurrent beat is also lower than the band gap energy by the same energy difference at room temperature.

The temperature dependence of the band gap energy and the resonance energy of the carriers contributing to the photocurrent beat is plotted in Fig. 3(c). Here, the band

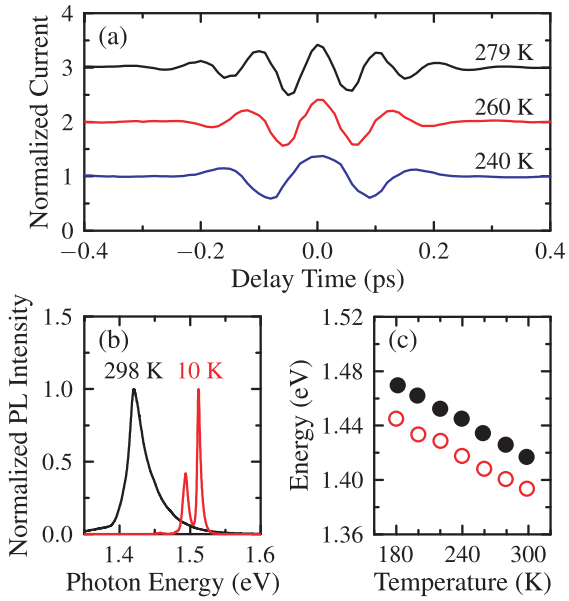

FIG. 3. (Color online) (a) Temperature dependence of normalized current under the in-phase condition. The temperature was set to 279, 260, and 240 K. (b) Normalized photoluminescence spectra at 298 (black line) and 10 (red line) K. (c) Temperature dependence of band gap energy (solid circles) and resonance energy of photocurrent beat (open circles).

gap energy is measured from the PL spectrum and the resonance energy is obtained from the photocurrent beat period using the method explained previously. With decreasing temperature, the resonance energy exhibits a blueshift similar to the temperature dependence of the band gap energy. The difference in the energies has a constant value of 26 meV for each temperature. Since this energy difference is consistent with the difference measured from the acceptor level at low temperature, it is found that the photocurrent beat is caused by the acceptor carriers. At high temperature above 100 K, it is difficult to measure the temperature dependence of the acceptor peak accurately using PL measurements, because of the overlapping of peaks; in contrast, the photocurrent beat measurement clearly reveals the resonance peak position for the range reaching room temperature. Therefore, this powerful technique can be used to measure the energy and dynamics of photocurrent generation sites in various materials including non-luminescent materials.

In order to understand the photocurrent beat mechanism, coherent control of a two-level system is considered theoretically. The density matrix for a two-level system is denoted by ρ_{ij}, where i and j are either the ground state, g, or the excited state, e. Since the photocurrent beat is caused by the acceptor level, the ground and excited states correspond to the acceptor level and conduction band, respectively. The excited states in the conduction band show slightly different resonance energies; this difference influences the system in the form of an inhomogeneous broadening of the resonance energy, which is discussed below. The equation of motion for the density matrix is expressed as $\partial\rho/\partial t = (-i/\hbar)[H,\rho]$, where H is composed of the unperturbed Hamiltonian, i.e., diagonal elements, $H_{gg} = \hbar\omega_{gg}$ and $H_{ee} = \hbar\omega_{ee}$, and the light-matter interaction Hamiltonian, i.e., off-diagonal elements, $H_{ge} = -\mu_{ge}E^*$ and $H_{eg} = -\mu_{eg}E$ [25–27]. In these matrix elements, $\hbar\omega_{gg}$ and $\hbar\omega_{ee}$ are the energies of the ground and excited states, respectively; μ_{ge} is the dipole moment of the transition, whose complex conjugate is denoted by μ_{eg}. The electric field of phase-locked pulses is expressed as $E = \sum_{j=1,2} E_j(t)e^{i\boldsymbol{k}\cdot\boldsymbol{r}-i\omega_{eg}(t-t_j)}e^{i\theta_j-i\omega_{ex}t_j}$, where $\boldsymbol{k}$ is the wave vector of excitation pulses and the energy difference, $\hbar\omega_{eg}$, is defined by $\hbar\omega_{ee} - \hbar\omega_{gg}$. In the spectrum of the excitation pulses, the electric field of the resonance energy, $\hbar\omega_{eg}$, is used for the optical transition. The phase lock is performed at the center frequency of the excitation pulses, ω_{ex}. The pulse shape, arrival time, and initial phase of the jth excitation pulse are denoted by $E_j(t)$, t_j, and θ_j, respectively. The relative phase, $\theta_{21} = \theta_2 - \theta_1$, is set to 0 ($\pi$) under the in-phase (out-of-phase) condition. The pulse shape, $E_j(t)$, is assumed to be a delta-function pulse: $a_j\delta(t - t_j)$ for simplicity, where a_j is the amplitude of the jth excitation pulse. To express the dynamics of density matrix, decay terms should be introduced in the equation of motion. The decay term with a time constant of T_1 (T_2) is assumed for diagonal (off-diagonal) matrix elements.

The excited-state population, $\rho_{ee}(t)$, is obtained by solving the equation of motion up to the second order of the excitation electric field, where we assume that the higher order terms are negligible because the photocurrent beat is observed independently of excitation intensity. Since the photocurrent magnitude is proportional to the excited-state population, the photocurrent is obtained from the time integral of $\rho_{ee}(t)$. In the above two-level system, the photocurrent induced by a localized state, i.e., an acceptor state, is calculated. In contrast, for an ensemble of localized states, the inhomogeneous broadening of the resonance energy is caused by the different excited states in the conduction band and the different local environments of the localized states. It is assumed to have a Gaussian distribution with a center energy of $\hbar\bar{\omega}_{eg}$ and a linewidth of $\hbar\sigma_i$. The photocurrent due to the localized states as a function of the delay time, $\tau = t_2 - t_1$, is expressed as

$$J_a(\tau) = \eta_a\left(a_1^2 + a_2^2\right) + 2\eta_a a_1 a_2 e^{-(\sigma_i^2/4)\tau^2} e^{-(1/T_2)|\tau|} \times \cos[(\omega_{ex} - \bar{\omega}_{eg})\tau - \theta_{21}], \quad (1)$$

where the photocurrent generation efficiency per the square of the amplitude of excitation pulse is denoted by η_a. The first term is the photocurrent due to single excitation pulses, where the current component, $\eta_a a_j^2$, is caused by the jth pulse. The second term represents the photocurrent beat, which is generated by both the first and second excitation pulses. The excited-state population is coherently controlled by the delay time between the excitation pulses. The beat period is determined by the detuning frequency, $\omega_{ex} - \bar{\omega}_{eg}$. The sign of the photocurrent beat is determined by the relative phase, θ_{21}, under the in-phase ($\theta_{21} = 0$) and out-of-phase ($\theta_{21} = \pi$) conditions. Coherent control of photocurrent is available within the time range before the first-generated polarization disappears. The time range is characterized by the dephasing time, T_2, and the time duration of free induction decay, $2/\sigma_i$, where the free induction decay factor, $e^{-(\sigma_i^2/4)\tau^2}$, is derived from the inhomogeneous broadening of the resonance energy. After exceeding the time range, the photocurrent becomes

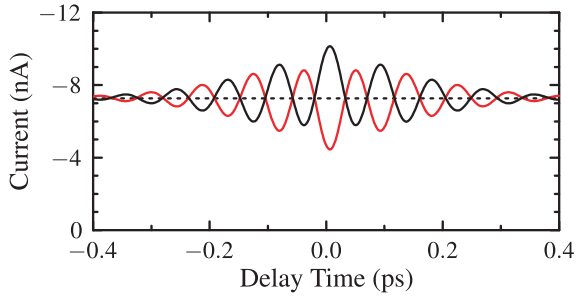

FIG. 4. (Color online) Calculated current as a function of the delay time under the in-phase (black line) and out-of-phase (red line) conditions. The result under the random-phase condition is represented by a dotted line.

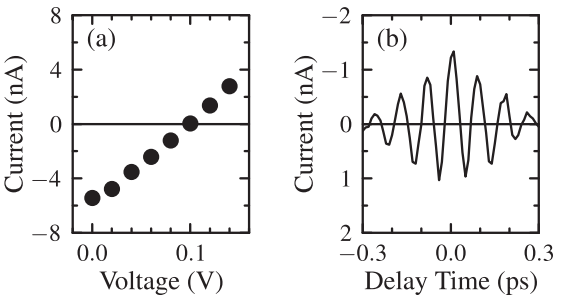

FIG. 5. (a) Voltage dependence of current for the delay time of 2.0 ps. (b) Current as a function of the delay time. The bias voltage was set to 0.1 V, and phase-locked pulses were set to in-phase.

independent of the delay time, because the first-generated quantum state cannot be changed by the second excitation.

In addition to the photocurrent due to the localized states, current components independent of the photocurrent beat should be taken into account. Since the carrier generation due to the band-to-band transition occurs resonantly, the photocurrent shows the delay-time dependence similar to Eq. (1), but without detuning. The photocurrent due to the band-to-band transition is expressed as

$$J_b(\tau) = \eta_b\left(a_1^2 + a_2^2\right) + 2\eta_b a_1 a_2 e^{-(\ln 2)\tau^2/\tau_p^2}\cos[-\theta_{21}], \quad (2)$$

where the photocurrent generation efficiency for the carriers due to the band-to-band transition is denoted by η_b. Since the inhomogeneous broadening of the continuum states in the band-to-band transition is determined by the spectral width of the excitation pulses, the free induction decay factor is expressed as $e^{-(\ln 2)\tau^2/\tau_p^2}$, where τ_p is a pulse duration. The remaining current components such as the steady-state current under the applied bias voltage and incoherent background photocurrent are independent of the delay time. They are collectively denoted by the constant, J_0. The total current is expressed as $J_a(\tau) + J_b(\tau) + J_0$, where the first, second, and third terms correspond to the current due to the acceptor excitation, the band-to-band transition, and the steady-state components, respectively.

The calculated results based on the above theoretical treatment are shown in Fig. 4, where the convolution of Eq. (1) and a Gaussian broadening function with a pulse duration of $\tau_p = 56$ fs is calculated; the slight shift of the center peak is the experimental error of the zero delay. The experimental photocurrent beat shown in Fig. 2(b) is successfully reproduced by the calculation. Here, the inhomogeneous broadening of acceptor levels, σ_i, is set to 7.3 ps^{-1}, which is estimated from the PL spectrum at 10 K. The interference contrast of the excitation pulses, $2a_1a_2/(a_1^2 + a_2^2) = 0.78$, is obtained from the interference intensity shown in Fig. 2(a). We verified that the dark current of the photodetector was negligibly small compared to the current intensity due to the excitation pulses; this value is determined only by the interference of two pulses. From the calculation, the dephasing time and current amplitudes are found to be $T_2 = 0.4$ ps, $2\eta_a a_1 a_2 = -2.3$ nA, $2\eta_b a_1 a_2 = -0.7$ nA, and $J_0 = -3.4$ nA. Note that the dephasing time is longer than that for the band-to-band transition, which has been reported to be a few ten femtoseconds [28]. The obtained value is comparable to the dephasing time of electron-hole pairs in quantum dots, which has been found to be a few hundred femtoseconds at room temperature [29,30]. This behavior, similar to the carriers in quantum dots, supports the conclusion obtained from the temperature dependence that the photocurrent beat is caused, not by the band-to-band transition, but by the localized acceptor states. Regarding the current amplitudes, the current induced by the acceptor states is large compared to that by the continuum states due to the band-to-band transition. The ratio of the carrier generation efficiency is obtained to be $\eta_a/\eta_b = 3.2$, where the carrier generation efficiencies for the acceptor states and the continuum states due to the band-to-band transition are denoted by η_a and η_b, respectively. The photocurrent is accurately decomposed into the acceptor-state and continuum-state components by comparing the current amplitudes.

The photocurrent beat can be used to control the photocurrent direction as follows. The voltage dependence of the current baseline is shown in Fig. 5(a), where the current baseline was measured at the delay time of 2.0 ps with total excitation intensity of 4.5 W/cm^2. Photoexcited carriers generate reverse current under unbiased condition, which can be suppressed by applying a positive bias. The current reaches zero at 0.1 V; at the balance voltage, the current direction becomes sensitive to slight changes in the number of carriers. Usually, the current direction is unchanged because the excitation intensity is fixed, but current direction control can be achieved by changing the delay time between the excitation pulses. The result of this coherent control at a balance voltage of 0.1 V is shown in Fig. 5(b). The photocurrent beat exhibits the flip of current direction at the center zero current, where the negative (positive) current corresponds to the current direction from the front to back (back to front) of the sample. This is the practical demonstration of directional photocurrent using coherent control of localized states at room temperature. Since the current direction is controlled by tuning the delay time only, this technique can be applied to ultrafast optical switching.

IV. CONCLUSION

We have demonstrated coherent control of photocurrent beat at room temperature. We found that the photocurrent beat

is caused by coherently controlled carriers of acceptor states within subpicosecond dephasing processes, and confirmed that this photocurrent beat measurement is an effective technique of characterization of current components. The photocurrent has been successfully classified into two different generation processes: localized-state and continuum-state carriers. Furthermore, we have achieved directional photocurrent control through applying an appropriate voltage.

Since the photocurrent dynamics are measured within the ultrafast regime, intrinsic material properties can be determined. This determination technique will reveal photocurrent composition in new materials, e.g., hidden localized levels which cannot be identified from optical measurements. The beat signal is also important to control the current direction. This simple technique can be applied to a wide range of materials.

ACKNOWLEDGMENTS

The authors would like to thank D. M. Tex and M. Okano for useful discussions. This work was supported by a Grant-in-Aid for JSPS Fellows and JST-CREST.

[1] M. A. Green, K. Emery, Y. Hishikawa, W. Warta, and E. D. Dunlop, Prog. Photovolt.: Res. Appl. **22**, 701 (2014).
[2] S. Niki, M. Contreras, I. Repins, M. Powalla, K. Kushiya, S. Ishizuka, and K. Matsubara, Prog. Photovolt.: Res. Appl. **18**, 453 (2010).
[3] S. Günes, H. Neugebauer, and N. S. Sariciftci, Chem. Rev. **107**, 1324 (2007).
[4] A. J. Nozik, Physica E **14**, 115 (2002).
[5] I. Gur, N. A. Fromer, M. L. Geier, and A. P. Alivisatos, Science **310**, 462 (2005).
[6] R. R. King, D. C. Law, K. M. Edmondson, C. M. Fetzer, G. S. Kinsey, H. Yoon, R. A. Sherif, and N. H. Karam, Appl. Phys. Lett. **90**, 183516 (2007).
[7] M. C. Beard, J. Phys. Chem. Lett. **2**, 1282 (2011).
[8] Y. Kanemitsu, Acc. Chem. Res. **46**, 1358 (2013).
[9] V. I. Klimov, Annu. Rev. Condens. Matter Phys. **5**, 285 (2014).
[10] M. B. Smith and J. Michl, Chem. Rev. **110**, 6891 (2010).
[11] D. N. Congreve, J. Lee, N. J. Thompson, E. Hontz, S. R. Yost, P. D. Reusswig, M. E. Bahlke, S. Reineke, T. Van Voorhis, and M. A. Baldo, Science **340**, 334 (2013).
[12] A. Luque, A. Martí, and C. Stanley, Nat. Photon. **6**, 146 (2012).
[13] D. M. Tex, I. Kamiya, and Y. Kanemitsu, Phys. Rev. B **87**, 245305 (2013).
[14] A. P. Heberle, J. J. Baumberg, and K. Köhler, Phys. Rev. Lett. **75**, 2598 (1995).
[15] M. U. Wehner, M. H. Ulm, D. S. Chemla, and M. Wegener, Phys. Rev. Lett. **80**, 1992 (1998).
[16] T. Voss, I. Rückmann, J. Gutowski, V. M. Axt, and T. Kuhn, Phys. Rev. B **73**, 115311 (2006).
[17] Y. Ogawa and F. Minami, Phys. Rev. B **75**, 073302 (2007).
[18] Y. Ogawa, H. Tahara, and F. Minami, Phys. Rev. B **87**, 165305 (2013).
[19] G. Kurizki, M. Shapiro, and P. Brumer, Phys. Rev. B **39**, 3435 (1989).
[20] A. Haché, Y. Kostoulas, R. Atanasov, J. L. P. Hughes, J. E. Sipe, and H. M. van Driel, Phys. Rev. Lett. **78**, 306 (1997).
[21] M. J. Stevens, A. L. Smirl, R. D. R. Bhat, A. Najmaie, J. E. Sipe, and H. M. van Driel, Phys. Rev. Lett. **90**, 136603 (2003).
[22] M. D. Sturge, Phys. Rev. **127**, 768 (1962).
[23] K. Kornitzer, T. Ebner, K. Thonke, R. Sauer, C. Kirchner, V. Schwegler, M. Kamp, M. Leszczynski, I. Grzegory, and S. Porowski, Phys. Rev. B **60**, 1471 (1999).
[24] D. J. Ashen, P. J. Dean, D. T. J. Hurle, J. B. Mullin, A. M. White, and P. D. Greene, J. Phys. Chem. Solids **36**, 1041 (1975).
[25] T. Yajima and Y. Taira, J. Phys. Soc. Jpn. **47**, 1620 (1979).
[26] H. Haug and S. W. Koch, *Quantum Theory of the Optical and Electronic Properties of Semiconductors*, 5th ed (World Scientific, Singapore, 2009).
[27] H. Tahara, Y. Ogawa, F. Minami, K. Akahane, and M. Sasaki, Phys. Rev. B **89**, 195306 (2014).
[28] P. C. Becker, H. L. Fragnito, C. H. Brito Cruz, R. L. Fork, J. E. Cunningham, J. E. Henry, and C. V. Shank, Phys. Rev. Lett. **61**, 1647 (1988).
[29] P. Borri, W. Langbein, J. Mørk, J. M. Hvam, F. Heinrichsdorff, M.-H. Mao, and D. Bimberg, Phys. Rev. B **60**, 7784 (1999).
[30] P. Borri, W. Langbein, S. Schneider, U. Woggon, R. L. Sellin, D. Ouyang, and D. Bimberg, Phys. Rev. Lett. **87**, 157401 (2001).